R. A. STAFF · P. DITCHFIELD · E. RHODES · J.-L. SCHWENNINGER
L. CLARK-BALZAN · S. LEE · R. N. E. BARTON

4. CHRONOLOGY

4.1 INTRODUCTION

The principal chronological method applied to the LSA Iberomaurusian units at Taforalt was radiocarbon (^{14}C) dating by Accelerator Mass Spectrometry (AMS), performed at the Oxford (UK) Radiocarbon Accelerator Unit (ORAU). Prior to AMS, all samples were chemically pre-treated to remove potential contaminants using standard ORAU protocols for each sample type (Brock/Higham/Ditchfield/Bronk Ramsey 2010). The technique was applied primarily to charcoals of short-lived woody plant species and the methods used for selecting and dating the samples from the site have been described elsewhere (Barton et al. 2013). These charcoals were identified by project wood specialists (R. Gale, D. Challinor and Y. Carrión Marco). A further programme of AMS ^{14}C dating of ostrich eggshell and bone samples was undertaken in parallel with the charcoal but was more restricted, due to the variable quality of collagen preservation and diagenesis of these materials. Significantly, the successfully assayed finds included dated human specimens and cut-marked bone from the burial area (Sector 10). Additionally, direct radiocarbon determinations on small seeds and other charred plant macrofossils were performed as part of a wider programme to identify the uses of food plants (Chapter 6), as well as to investigate the stratigraphic integrity of the deposits.

Luminescence dating was also applied to the cave sediments and to a limited number of burnt cherts in the Iberomaurusian units. The methodology for Optically Stimulated Luminescence (OSL) dating of sediments has been described elsewhere (Clark-Balzan et al. 2012; Clark-Balzan 2013), as have the Thermoluminescence (TL) methods on burnt cherts (Rhodes in Bouzouggar et al. 2007). For the OSL dating, metal tubes were hammered into the sections and sand-sized quartz mineral grains were extracted from these samples for measurement. Selected burnt worked cherts were taken for TL dating which entailed wrapping the specimens in aluminium foil immediately upon excavation and obtaining small sediment samples adjacent to the finds for external gamma dose rate determination by neutron activation analysis (NAA) or a combination of inductively coupled plasma mass spectrometry (ICP-MS) and inductively coupled plasma atomic emission spectrometry (ICP-AES). Not all of the luminescence results are reported below. In particular, many of the OSL ages were found to be consistently older than either the TL or the AMS ^{14}C ages. A potential source of error may be associated with the effects of severe burning on the sediment constituents and difficulties in establishing a reliable dose rate. Suspected post-depositional alterations in the chemical composition of the ashy sediment are the subject of continuing investigation.

A third dating method employed at Taforalt was that of tephrochronology. The technique is relatively new and has not yet been widely applied to sites in North Africa (Barton et al. 2015). The method depends on geochemically identifying microscopic vitreous shards (tephra) ejected by individual explosive volcanic eruptions and dispersed through the atmosphere (Lowe 2011). With greater distance from the source volcanoes of these eruptions, the fallout of tephra reduces. Therefore, at distal sites such as Taforalt (there being no known volcanoes close to Taforalt active in the Quaternary), tephra shards are deposited in very low abundances but may, nevertheless, still be identified as non-visible (to the naked eye) concentrations of 'cryptotephra'. So long as the geochemistry of a tephra shard is sufficiently unique, its 'geochemical fingerprint'

can be used to identify isochronous markers across potentially large geographic distances (as well as small distances within individual sites), providing tie-points to other distal archaeological or palaeoenvironmental sites, as well as to the ultimate volcanic source. Thus, chronological information from proximal volcanic material, or from other distal sites, can be integrated using these tephra isochrons. Whilst tephra fallout across space can be thought of as contemporaneous with (i. e. generally, within a year of) the eruptive episode, subsequent taphonomic re-working of the primary ashfall can be an issue, and must also be taken into account.

4.2 AMS RADIOCARBON DATING

AMS radiocarbon dating was undertaken in each of the main sectors yielding LSA finds (Sectors 8, 3, 6, 9 and 10). The results are presented by Sector, and discussed in this sequence below. Following radiocarbon convention, all raw radiocarbon determinations are presented as 'BP' ('Before Present', where present is defined as 1950 CE) with calibrated radiocarbon ages given on the current best-estimate calendar timescale in 'calibrated years Before Present' ('cal BP'). It should be noted that throughout this present volume the radiocarbon calibration curve 'IntCal13' (Reimer et al. 2013) has been used (cf. the previous iteration of the calibration curve, 'IntCal09', Reimer et al. 2009, that was applied in previous publications on Taforalt, *inter alia*, by Barton et al. 2013).

Sector 8

The entire stratigraphic sequence in Sector 8 covers a thickness of 5.55 m. A total of 52 radiocarbon determinations (including three duplicated assays) on charcoals and cut-marked bones (collagen fraction) had been previously published from the Iberomaurusian levels in this sector (Barton et al. 2013). The majority of these samples were on individual large charcoal fragments identified to species (**tab. 4.1**). A further 11 AMS radiocarbon determinations from the same profile have been obtained subsequently and are included here. They consist of measurements on eight bone and three charcoal specimens.

The radiocarbon data were subjected to Bayesian statistical modelling (**fig. 4.1** and **tab. 4.1**). This is a well-established tool for combining acquired information (*prior probability*) with chronological measurements (*likelihoods*) to improve the precision and accuracy of the site's chronology (*posterior probability*). We used the freely available computer software OxCal v.4.2 (Bronk Ramsey 2017) for such analysis. Briefly, the Bayesian model in the present case consisted of four separate Poisson process ('**P_Sequence**') deposition models (Bronk Ramsey 2008) – one for the Grey Series and three for the underlying Yellow Series (**fig. 4.1**). The model averaging approach of Bronk Ramsey/Lee (2013) was utilised to independently estimate the optimal rigidity of these **P_Sequences** (i. e. the variability in deposition rate, defined by the '**k**' parameter in OxCal). The Yellow Series was split into three separate **P_Sequences** due to empirically observed breaks (hiatuses) down the list of dates (i. e. from the radiocarbon data themselves, rather than anything sedimentologically observable at the site).

The precise position (represented by 'nominal depth') of samples in the sequence included some uncertainty (ranging from ± 1 cm to ± 16 cm) when transferring positions onto the single composite depth scale for the Sector, as described in **Chapter 2**. This was accounted for in the Bayesian modelling by placing the individual radiocarbon dated samples in a series of individual sequences, between corresponding upper and lower

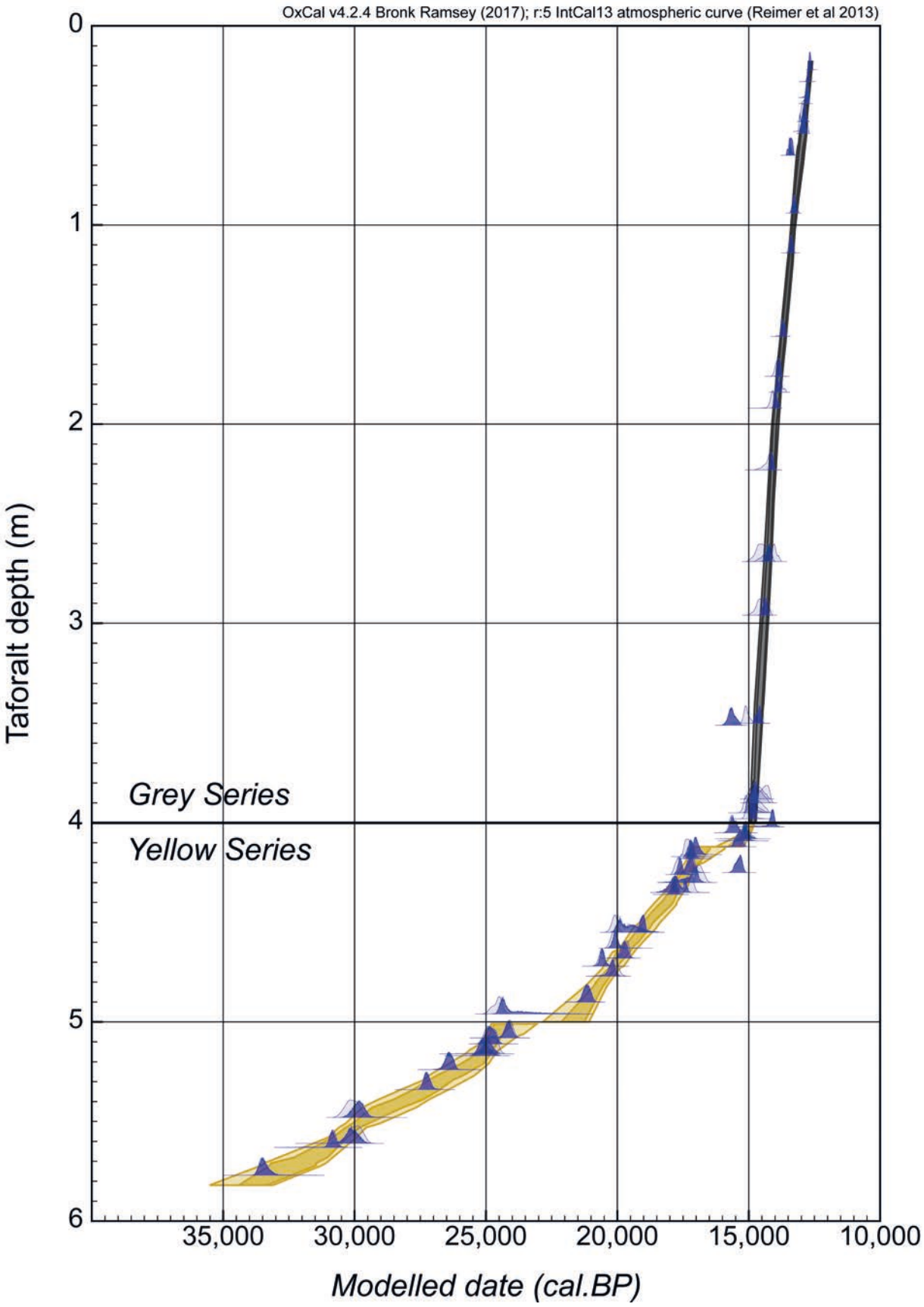

Fig. 4.1 Bayesian age-depth model of AMS ^{14}C data for Taforalt cultural sequence; the posterior 68.2 % and 95.4 % uncertainty envelopes are plotted in grey and gold for the GS and YS, respectively; note that the y-axis represents *nominal* depth measurements.

ORAU lab code	Conventional ^{14}C age BP (± 1σ)	Calibrated age (cal BP) 95.4 % range	Modelled† age (cal BP) 95.4 % range	Unit	Nominal depth†† (m)	Species	<TAF Ref>
OxA-24111	10,680 ± 45	12,566-12,713	12,611-12,725	L2	0.18-0.26	*Ammotragus lervia*	TAF09-7319
OxA-34434	10,855 ± 50	12,686-12,814	12,688-12,788	G88	0.18-0.38	*Quercus* sp.	TAF03-200a
OxA-13479	10,935 ± 40	12,705-12,900	12,720-12,828	G88	0.31-0.41	*Pinus* sp.	TAF03-200b
OxA-23404	10,870 ± 45	12,693-12,813	12,700-12,817	L3	0.26-0.52	*Pinus* sp.	TAF09-7525
OxA-13480	10,950 ± 45	12,711-12,950	12,730-12,866	G89	0.34-0.44	*Pinus* sp.	TAF03-202
OxA-13516	11,065 ± 45	12,799-13,059	12,798-12,985	G89	0.43-0.53	*Pinus* sp.	TAF03-203
OxA-24112	11,165 ± 45	12,905-13,125	12,804-13,045	L4	0.52-0.54	*Ammotragus lervia*	TAF09-7997
OxA-13517	10,990 ± 45	12,730-12,990	12,819-13,010	G90	0.49-0.59	Dicotyledonous	TAF03-204
[a]OxA-24113	11,540 ± 50	13,281-13,468	13,280-13,467	L6	0.61-0.69	*Gazella*	TAF09-8289b
[a]OxA-23405	11,615 ± 50	13,329-13,562	13,330-13,562	L6	0.61-0.69	*Juniperus*/ *Tetraclinus*	TAF09-8275
OxA-27276	11,410 ± 55	13,123-13,384	13,169-13,344	L8	0.86-1.02	*Ammotragus lervia*	TAF09-8552
OxA-23407	11,465 ± 50	13,193-13,435	13,200-13,354	L8	0.86-1.02	*Juniperus*/ *Tetraclinus*	TAF09-8590#
OxA-23406	11,445 ± 55	13,151-13,420	13,200-13,354	L8	0.86-1.02	*Juniperus*/ *Tetraclinus*	TAF09-8590#
OxA-23408	11,545 ± 55	13,275-13,476	13,310-13,467	L11	1.09-1.19	*Pinus* sp.	TAF09-8849
OxA-23409	11,890 ± 55	13,555-13,828	13,590-13,780	L15	1.52-1.60	*Pinus* sp.	TAF10-9159
OxA-27277	12,040 ± 55	13,754-14,051	13,750-13,945	L17	1.71-1.81	*Ammotragus lervia*	TAF10-9368
OxA-27278	11.945 ± 55	13,590-13,976	13,780-13,989	L19	1.81-1.86	*Ammotragus lervia*	TAF10-9484
OxA-27281	12,210 ± 55	13,925-14,312	13,831-14,077	L20	1.86-1.99	*Ammotragus lervia*	TAF10-9578
OxA-27280	12,290 ± 55	14,033-14,600	13,999-14,233	L23	2.07-2.39	*Ammotragus lervia*	TAF10-9775
[c]OxA-27279	12,310 ± 55	14,064-14,649	14,135-14,423	L24	2.51-2.86	*Ammotragus lervia*	TAF10-9881
[c]OxA-34435	12,420 ± 55	14,177-14,855	14,147-14,421	G96-2	2.61-2.77	*Pinus* (charred seeds)	TAF03-G96-2A
[c]OxA-34436	12,145 ± 55	13,815-14,177	14,131-14,421	G96-2	2.61-2.77	*Pinus* (charred seeds)	TAF03-G96-2B
[c]OxA-23410	12,405 ± 55	14,156-14,855	14,244-14,545	L25	2.92-3.00	*Juniperus*/ *Tetraclinus*	TAF10-10052
[b]OxA-13477	12,675 ± 50	14,829-15,271	14,483-14,810	G97	3.40-3.60	Conifer	TAF03-36

Tab. 4.1 Sector 8 (and inward continuation): radiocarbon data. OxCal v.4.2 Bayesian Modelling; †† for explanation of "nominal depth", see **Chapter 2**. – All calibration has been produced using IntCal13.

Same sample measured twice.

* Plausibly a date on a Y1 object physically disturbed and drawn down into Y2 during very obvious plastic deformation affecting the contact zone between the two units (note also apparent mixing of lithic artefacts at this level).

** Uncertain (Y2 or Y4?); relative depth for ordering/modelling estimated from actual surveyed depth.

[a] Samples plausibly displaced from their original position (also yielding posterior outlier probabilities of > 95 % in the modelling); [b] Samples possibly displaced from their original position (also yielding posterior outlier probabilities > 50 % in the modelling); [c] Particularly stony units (clast-supported) in the centre of the Grey Series (with highest sedimentation rates expected; less reliable contexts for tiny objects like charred seeds).

ORAU lab code	Conventional ^{14}C age BP (± 1σ)	Calibrated age (cal BP) 95.4 % range	Modelled† age (cal BP) 95.4 % range	Unit	Nominal depth†† (m)	Species	<TAF Ref>
[a]OxA-23411	13,060 ± 65	15,345-15,895	15,339-15,902	L28	3.42-3.60	*Juniperus*/ *Tetraclinus*	TAF10-10319
OxA-13478	12,495 ± 50	14,314-15,052	14,664-14,924	G99	3.78-3.98	Juniperus/ Tetraclinus	TAF03-90
OxA-22902	12,370 ± 50	14,129-14,740	14,658-14,927	G99 sqD17	3.80-4.00	Conifer	TAF08-6834
OxA-22904	12,490 ± 50	14,303-15,052	14,670-14,930	G99	3.80-4.00	Conifer	TAF08-6840
OxA-22787	12,545 ± 55	14,443-15,131	14,710-14,955	G99	3.85-4.05	Conifer	TAF08-6841
OxA-22785	12,500 ± 55	14,313-15,066	14,716-14,956	G99 sqD17	3.85-4.05	cf. *Juniperus*	TAF08-6833#
OxA-22784	12,660 ± 70	14,731-15,285	14,716-14,956	G99 sqD17	3.85-4.05	cf. *Juniperus*	TAF08-6833#
OxA-24109	12,605 ± 55	14,684-15,199	14,734-14,970	G100	3.88-4.08	Bos	TAF04-466
		(Grey/Yellow Boundary)	(Irregular Diachronic Erosion Event)				
OxA-22786	12,200 ± 55	13,910-14,292	13,853-14,788	Y1 sqD17	3.92-4.12	cf. *Juniperus*	TAF08-6836
OxA-22903	13,045 ± 50	15,356-15,838	15,320-15,808	Y1 sqD17	3.95-4.15	cf. *Cedrus*	TAF08-6835
OxA-22905	12,665 ± 50	14,806-15,256	14,933-15,289	Y1	4.03-4.13	cf. *Arbutus*	TAF08-6842
OxA-14349	12,690 ± 55	14,844-15,299	14,855-15,306	Y1	3.98-4.18	*Struthio* (ostrich eggshell)	TAF04-657
OxA-27282	12,730 ± 60	14,908-15,365	14,940-15,368	L30	4.00-4.18	*Alcelaphus* sp.	TAF10-10710
OxA-22788	12,850 ± 55	15,144-15,576	15,180-15,615	Y1	4.07-4.17	Conifer	TAF08-6844
		(Major Erosion Event)					
OxA-16267	14,005 ± 60	16,716-17,256	16,745-17,214	Y2	4.11-4.21	Tetraclinus articulata	TAF06-5415
OxA-22907	14,230 ± 55	17,120-17,523	16,964-17,446	Y2	4.12-4.22	cf. *Juniperus*	TAF08-6853
OxA-22906	14,135 ± 55	16,996-17,437	16,972-17,380	Y2	4.13-4.23	Conifer	TAF08-6852
OxA-22908	14,110 ± 55	16,954-17,413	17,009-17,447	Y2	4.20-4.30	cf. *Arbutus*	TAF08-6854
[a]OxA-27283	12,875 ± 60	15,160-15,618	15,157-15,614	L31*	4.20-4.30	*Equus* sp.	TAF10-10847
OxA-16268	14,515 ± 60	17,500-17,903	17,273-17,817	Y2	4.21-4.31	Tetraclinus articulata	TAF06-5416
OxA-13519	13,905 ± 55	16,585-17,075	16,765-17,906	Y2	4.20-4.40	*Juniperus*/ *Tetraclinus*	TAF03-317
[b]OxA-22909	14,140 ± 55	17,004-17,443	17,307-18,231	Y2	4.30-4.40	Conifer	TAF08-6855
OxA-16272	14,630 ± 60	17,621-17,995	17,652-18,010	Y2	4.31-4.41	*Quercus* sp.	TAF06-5421
OxA-16269	15,790 ± 60	18,882-19,217	18,886-19,236	Y2	4.50-4.60	*Juniperus* sp.	TAF06-5417
[b]OxA-14350	16,660 ± 70	19,880-20,337	18,862-20,136	Y2 spit5A	4.45-4.65	*Struthio* (ostrich eggshell)	TAF04-1734
OxA-14351	16,695 ± 70	19,925-20,378	19,760-20,347	**	4.53-4.73	*Struthio* (ostrich eggshell)	TAF04-1927

Tab. 4.1 (continued)

ORAU lab code	Conventional ^{14}C age BP (± 1σ)	Calibrated age (cal BP) 95.4 % range	Modelled† age (cal BP) 95.4 % range	Unit	Nominal depth†† (m)	Species	<TAF Ref>
OxA-16270	16,285 ± 65	19,477-19,908	19,514-19,993	Y3	4.63-4.73	*Pinus* sp.	TAF06-5418
OxA-13518	17,085 ± 65	20,404-20,835	20,309-20,807	Y3	4.62-4.82	*Quercus* sp.	TAF03-316
OxA-16242	16,630 ± 75	19,826-20,315	19,940-20,643	Y4	4.72-4.82	Dicot unidentified	TAF06-5419
OxA-16273	17,515 ± 75	20,894-21,430	20,882-21,436	Y4	4.80-5.00	*Pinus* sp.	TAF06-5422
		[LSA/MSA transition]					
OxA-16271	20,420 ± 90	24,253-24,945	22,293-24,635	Y4	4.91-5.01	*Pinus* sp.	TAF06-5420
		(Minor Erosion Event)					
OxA-16274	20,630 ± 90	24,499-25,192	24,514-25,152	Y5	5.06-5.16	Conifer	TAF06-5424

Tab. 4.1 (continued)

Boundaries delineating the total depth uncertainty for those samples. These upper and lower Boundaries were then cross-referenced into the four primary P_Sequences.

Duplicate measurements were combined using the R_Combine function in OxCal to produce a weighted average. Objective outlier analysis was also utilised to account for potential statistical outliers in the radiocarbon data. The 'General' outlier model of Bronk Ramsey (2009) was applied, accounting for errors in the calendar age scale of samples (i. e. primarily issues of residuality or intrusion within the deposition environment). Additionally, the 'SSimple' outlier model was applied to the duplicate measurements within the R_Combine functions (Bronk Ramsey 2009). All samples were assigned a prior outlier probability of 5 %, since there was no reason *a priori* to believe that any samples were more likely to be erroneous than others.

The modelled chronology for the Iberomaurusian sequence in Sector 8 is reproduced in table 4.1. In terms of the outlier analyses applied, four samples (OxA-17283, OxA-23405, OxA-24113 and OxA-23411) yielded posterior outlier probabilities of >95 %, and were therefore excluded from the final model (presented here). A further 3 samples gave posterior outlier probabilities >50 % (OxA-14350, OxA-22909 and OxA-13477).

The boundary between the Yellow and Grey Series dates to shortly after 15,000 cal BP (base of GS 14,966-14,733 cal BP; top of YS 15,070-14,767 cal BP; 95.4 % ranges) according to our revised Bayesian modelling against IntCal13, and should be considered as superseding the modelling presented by Barton et al. (2013). The overall picture gained from Bayesian modelling of the S8 radiocarbon dataset, through both the YS and GS, supports the basic plotting of the calibrated dates shown in figure 2.17. We conclude that our understanding of the chronology of the S8 sequence is robust.

Sector 3

This sector is separated from Sector 8 by both Ruhlmann's south trench and Roche's subsequently excavated northwards notch. The dates presented by Roche (1976) are not considered reliable enough for making direct comparisons. However, our new AMS ^{14}C dates (tab. 4.2) confirm the interpretation of the linkage between Sectors 3 and 8. The lowermost two ^{14}C samples relate to units containing pre-Iberomaurusian finds.

ORAU lab code	Conventional ^{14}C age BP (± 1σ)	Calibrated age (cal BP) 95.4 % range	Unit	Species	<TAF Ref>
OxA-26484	13,980 ± 80	17,254-16,620	4-6	*Cupressus* sp. or *Juniperus*	TAF08-5820
OxA-26639	14,800 ± 60	18,204-17,824	11-13, top RXII	*Prunus* sp.	TAF08-6159
OxA-16264	15,355 ± 65	18,781-18,471	22, RXII = Y3	*Quercus* sp.	TAF06-5412
OxA-16265	15,585 ± 65	18,976-18,692	30, RXII = Y3	*Pinus halepensis*	TAF06-5413
OxA-26640	16,170 ± 65	19,726-19,278	28-30	*Cupressus* sp.	TAF08-6633#
OxA-26641	16,165 ± 65	19,717-19,272	28-30	*Cupressus* sp.	TAF08-6633#
OxA-26642	16,030 ± 65	19,561-19,140	30-32, RXIII mid	*Juniperus*/*Tetraclinus*	TAF08-6646
OxA-26643	17,070 ± 75	20,832-20,355	38-40, RXIII base	*Juniperus*/*Tetraclinus*	TAF08-6705
OxA-16266	20,500 ± 90	25,044-24,350	58, RXIV = Y5	Conifer cf. *Cupressus*	TAF06-5414
OxA-26644	22,580 ± 110	27,238-26,541	58-60, RXIV mid	*Pinus* sp.	TAF08-6858

Tab. 4.2 AMS ^{14}C data for Sector 3. # Sample measured twice.

ORAU lab code	Conventional ^{14}C age BP (± 1σ)	Calibrated age (cal BP) 95.4 % range	Unit	Species	<TAF Ref>
OxA-16263	13,975 ± 60	17,196-16,670	S6-(N)2	*Juniperus* sp.	TAF06-5411
OxA-16262	15,995 ± 65	19,526-19,081	S6-(N)6	*Pinus* sp.	TAF06-5410

Tab. 4.3 AMS ^{14}C data for Sector 6.

Sector 6

The units dated here belong to the Upper Laminated group but it is not yet certain how, or even if, they correlate with the sequence in the Raynal type-section in Sector 1.

Sector 9

Six AMS radiocarbon determinations relate to the dating of the Iberomaurusian in Sector 9. They comprise five dates on charcoal and one on ostrich eggshell. The two charcoal dates from Units U1 and U2 (OxA-16260 and OxA-16240) come from the inner, west end of S9 and lie stratigraphically above CTX9 at the east

ORAU lab code	Conventional ^{14}C age BP (± 1σ)	Calibrated age (cal BP) 95.4 % range	Unit	Species	<TAF Ref>
OxA-16260	18,005 ± 75	21,559-22,058	S9-U1	*Tetraclinus articulata*	TAF06-5407
OxA-16240	18,185 ± 75	21,825-22,292	S9-U2	Charcoal unidentified	TAF04-1133
OxA-35508	16,410 ± 70	19,583-20,025	S9-CTX5	*Pinus* cf. *pinaster*	TAF16-14786
OxA-35993*	16,670 ± 55	19,915-20,318	S9-CTX6	*Struthio*	TAF16-14995
OxA-35509	19,230 ± 80	22,912-23,459	S9-CTX9	*Pinus* sp.	TAF16-15374
OxA-36628	18,505 ± 80	22,166-22,569	S9-CTX10	*Juniperus*/*Tetraclinus*	TAF17-15921

Tab. 4.4 AMS ^{14}C data for Sector 9. *ostrich eggshell dates problematic.

(outer) end of the Sector 9 trench. The charcoal from the base of CTX9 (OxA-35509) is so far the oldest date for the Iberomaurusian at Taforalt. CTX10 is a hearth-like band that lies a little higher, within CTX9, therefore explaining its younger age. The dates on ostrich eggshell from CTX6 (OxA-35993) and charcoal from the CTX5 (OxA-35508) appear to be too young. There is a systematic problem in dating ostrich eggshell at this site. The charcoal date in CTX5 is from the truncated top of the outer, east end of S9, and is suspected as coming from a disturbed context.

Sector 10

Bone and charcoal samples for dating were collected from near the back of the cave in the grey ashy deposits (Grey Series). They comprise human remains from burials (all excavated during the present campaign) plus cut-marked specimens of Barbary sheep (OxA-15441; OxA-15442; OxA-15443) and Ephedra charcoals (OxA-29263; OxA-29264). Although not demonstrably associated with individual burials, the animal bone shows signs of deliberate modification (butchery) and comes from broadly the same sedimentary contexts as the assemblage of human remains. The same is true of the Ephedra specimens. A dated bovid metatarsus shaft fragment (OxA-16688) was recovered from near one of the multiple burials (which includes Individual 4), but from a slightly higher level and in association with further human bones (in which no collagen is preserved). Another one of the Barbary sheep (*Ammotragus*) bones (OxA-24645) is reliably associated with human Individual 5.

Duplicate measurements were undertaken on two samples. OxA-X-2193-45 had a low collagen yield (6.0 mg from 1300 mg starting weight, i. e. 0.46 % yield compared to the ORAU quality assurance threshold of 1 % collagen yield, hence the 'OxA-X-' prefix). The repeat sub-sample, OxA-16688 (yielding 80 mg collagen from 3000 mg starting weight), produced a statistically indistinguishable result. Likewise, OxA-16663 was

ORAU lab code	Conventional ^{14}C age BP (± 1σ)	Calibrated age (cal BP) 95.4 % range	Species	<TAF Ref>
OxA-15441	12,325 ± 50	14,660-14,086	Ovicaprid	TAF05-2530
OxA-15442	12,400 ± 50	14,817-14,156	Ovicaprid	TAF05-3152
OxA-15443	12,310 ± 60	14,670-14,058	Unident. bone	TAF05-3201
OxA-24645	12,305 ± 60	14,662-14,052	*Ammotragus*	TAF08-6716
OxA-27284	12,520 ± 55	15,101-14,365	Canid	TAF10-11398
OxA-X-2193-45	12,590 ± 70	15,211-14,499	Bovid	TAF06-4124#
OxA-16688	12 475 ± 50	15,015-14,275	Bovid	TAF06-4124#
OxA-16663	12,470 ± 100	15,086-14,189	*Homo* Ind 7	TAF06-4797#
OxA-16689	12,485 ± 80	15,080-14,241	*Homo* Ind 7	TAF06-4797#
OxA-23660	12,380 ± 55	14,783-14,130	*Homo* Ind 4	TAF08-5566
OxA-23778	12,265 ± 50	14,468-14,005	*Homo* Ind 5	TAF08 6999
OxA-23779	12,255 ± 50	14,431-13,993	*Homo* Ind 6	TAF08 5733
OxA-23780	12,355 ± 50	14,712-14,116	*Homo* Ind 9	TAF09 8260
OxA-23781	12,410 ± 50	14,846-14,168	*Homo* Ind 14	TAF09 9103#
OxA-23782	12,460 ± 55	14,995-14,242	*Homo* Ind 14	TAF09 9103#
OxA-29263	12,410 ± 50	14,846-14,168	*Ephedra*	TAF13 12047
OxA-29264	13,065 ± 55	15,886-15,372	*Ephedra*	TAF13 12264

Tab. 4.5 AMS ^{14}C data for Sector 10. # Sample measured twice.

Type	Lab code	Age (± 1σ)	Unit	<TAF Ref>
OSL	X1867	19,300 ± 1200	Grey Series	TAF03-[OS]L16
OSL	X1864	21,700 ± 1300	Yellow Series Y2spit4	TAF03-[OS]L13
TL	X2259 [ANU:K0338]	17,400 ± 700	Grey Series G100	TAF04-762
TL	X1866 [ANU:K0317]	19,100 ± 1200	Grey Series base	TAF03-328 ([T]L15)

Tab. 4.6 OSL and TL ages for Sector 8 relevant to LSA units. – (After E. J. Rhodes in: Bouzouggar et al. 2007).

repeated because of a low collagen yield (3.0 mg from 100 mg starting weight, as compared to a further ORAU quality assurance stipulation that collagen yield should exceed 5.0 mg as well as the 1 % threshold). The second determination (OxA-16689) also yielded relatively little collagen (4.7 mg from 260 mg starting weight), but again provided a statistically indistinguishable measurement. For all four of the above sub-samples, the C:N ratios (providing an indication of whether or not any contamination had been successfully chemically removed from the remaining collagen) were acceptable (i. e. within the acceptable range of between 3.00 and 3.45, according to ORAU protocol).
The dated human bones relate to a number of different individuals: OxA-16663 is from Individual 7; OxA-23660, Individual 4; OxA-23778, Individual 5; OxA-23779, Individual 6; OxA-23780, Individual 9; and OxA-23781 and OxA-23782 (a duplicated sample), Individual 14. These are further discussed in **Chapter 15**.

4.3 LUMINESCENCE DATING

Sector 8

Sampling in the early stages of the project in 2003 was undertaken by ER and provided two OSL dates on sediments and two TL age determinations on burnt chert artefacts in Sector 8 (**tab. 4.6** and Barton et al. 2007, fig.15.2). The luminescence dating methods taken together have produced a set of results which is internally consistent. However, the dates from the Grey Series are at odds with the results of the radiocarbon dating, and this will be further referred to in the discussion at the end of this chapter.

Sector 3

Of the OSL samples from Sector 3, two were located in the Iberomaurusian sequence above the distinctive Y5 marker horizon (see **Chapter 2**). The results are presented in **table 4.7** and are considered slightly older than the AMS radiocarbon dates in the same sequence.

Sample	Multigrain Age (ka) (± 1σ)	Single Grain Age (ka) (± 1σ)	Unit
X3362 [OSL-TAF08-13]	20.0 ± 1.7	18.2 ± 1.4	S3-AOH09[8-29]
X3361 [OSL-TAF08-12]	22.9 ± 2.2	20.2 ± 1.8	S3-AOH09[40-44]

Tab. 4.7 Sector 3 OSL ages for Iberomaurusian levels. – (After Clark-Balzan 2013).

Sample	K (%)	Th (ppm)	U (ppm)	Gamma Dose Rate* (Gy ka^{-1})	Depth (cm)**	Cosmic Dose Rate (Gy ka^{-1})	Total Wet Dose Rate (Gy ka^{-1})	Age (ka)
OSL-TAF09-20	1.58	5.6	1.6	0.55 ± 0.03	35-45	0.094 ± 0.009	1.87 ± 0.13	18.6 ± 1.7
OSL-TAF09-21	0.96	4.3	1.3	0.57 ± 0.03	70-80	0.091 ± 0.008	1.45 ± 0.09	25.1 ± 2.3

Tab. 4.8 Sector 9 values for dose rate calculations and final ages – (sample depth ranges are in cm below surface).
* Determined on site with a portable gamma-ray spectrometer calibrated against the Oxford blocks (Rhodes/Schwenninger 2007).
** The original burial depth of both samples is likely to have been in excess of 3 m due to the removal of substantial amounts of sediment during previous excavations by Ruhlmann & Roche.

Sector 9

OSL samples were taken from Sector 9 by LC-B. Sampling was from one of the cleaned vertical sections at the eastern end of Ruhlmann's north trench and was focused on units in which lithic artefacts and charcoals were present. Lithic artefacts identifiable as Iberomaurusian were recorded only from the top sample at 35-45 cm. The lithostratigraphy is described in Chapter 2.

4.4 CRYPTOTEPHRA (SECTOR 8)

Cryptotephra was recovered in low concentrations throughout the top 18 cm of the Yellow Series, in Unit Y1, Sector 8 (Barton et al. 2015, fig. 4). The sediments here have been radiocarbon dated to between 14.8 and 17.2 ka cal BP. Glass shards display elongated vesicles and fluted structures and are the largest so-far observed from the site, with longest axis lengths of up to 100 µm. As an initial test of whether the 18 cm spread of tephra was all from the same eruption, two samples from within this depth range were picked and analysed. The samples returned matching rhyolitic compositions (Barton et al. 2015, tabs 1-2). The sediments of Y1 are characterised by finely laminated, fine to medium sands, indicating emplacement by gentle wash processes. The distribution of the tephra and the homogeneous composition therefore likely reflects the time over which these tephra shards continued to be re-worked (washed/blown) into the cave from the catchment, following a single volcanic eruption.
The major and minor element composition of this rhyolitic tephra is similar to that observed in tephras from potentially diverse geographic source regions. For example, multiple similar rhyolitic tephras from Icelandic and Aeolian volcanoes have been described from distal localities in this time-frame (Davies et al. 2012; Albert et al. 2012). Based upon major element geochemistry, similarities are seen between TAF-S8-Y1 and the Icelandic Penifiler and Borrobol tephra layers (13,939 ± 66 cal BP and 14,098 ± 47 cal BP, respectively (Bronk Ramsey et al. 2015), i. e. slightly post-dating the modelled age of the tephra in Taforalt), as well as the Lipari Gabelotto Fiumibianco from the Aeolian Islands. However, comparison of the limited available trace element geochemistry data shows that tephra from both of these sources is distinctly different from TAF-S8-Y1 (Barton et al. 2015), and the tephras from Iceland are currently not identified beyond NW Europe. The size and abundance of shards do not necessarily reflect distance from source: the relationship is not particularly straightforward as the magnitude of the eruption, height of the plume, and the strength and direction of the wind will control tephra dispersal and deposition, whilst taphonomic processes govern the preservation.

That said, longest axis lengths of up to 100 µm is a characteristic likely ruling out an Icelandic source. The source of the cryptotephra in TAF-S8-Y1, for the present, remains unknown.
Cryptotephra has also been located in various units of Sector 9 (Victoria Smith, pers. comm.). This is currently under investigation.

4.5 DISCUSSION

The key sequence for the Iberomaurusian at Taforalt is in Sector 8 for which we have obtained 63 ^{14}C determinations. This comprises two main sediment units: the upper part of the Yellow Series (YS) and the Grey Series (GS). Overall, the GS represents a rapid sediment accumulation brought about by a significant increase in anthropogenic activity in the cave. Our dating evidence suggests a commencement in GS deposition within a couple of centuries of 15,000 cal BP, although it has to be remembered that the GS has an irregular and erosive base and this is corroborated by variation in dating results of the undulating surface of this deposit. The youngest age from the top of the GS (and by definition related to Iberomaurusian occupation) is given by a Barbary sheep phalange at 10,680 ± 45 BP (12,568-12,713 cal BP at 95.4 % probability). However, it cannot be ascertained exactly when human activity ceased at the site because the top of the deposits were removed by the military authorities in 1939 (see **Chapter 1**). The dates confirm a rapid deposition rate in the GS, generally faster in the lower parts and slowing somewhat towards the top.
In the YS a much slower accumulation rate is recorded, as shown by sediment analysis and confirmed by AMS ^{14}C dating. Another point worth highlighting is that the oldest preserved Iberomaurusian deposits occur, not in Sector 8, but on the opposite side of the cave in Sector 9 (**tab. 4.4**). The latter deposits form part of a 'local' sequence that cannot be correlated directly with the units in Sector 8. As discussed in **Chapter 2**, we suspect that the marginally earlier dates in Sector 9 are probably due to better distinguishability from our perspective, the slight differences in sedimentary accumulation modes and rates on either side of the cave having left the S9 sequence less condensed than in S8. In any case, the LSA Iberomaurusian deposits began to accumulate sometime between 22,912-23,459 cal BP (at 95.4 % confidence) (**tab. 4.4**).
Finally, one issue that we cannot yet resolve is the apparently systematic discrepancy between some of the luminescence and AMS ^{14}C dating results. This is especially pronounced in the Grey Series in Sector 8 which, as has previously been mentioned, consists dominantly of burnt sediment and ash. TL and OSL dates obtained from samples collected within the Grey Series appear to systematically overestimate the true depositional age by more than 2000 years. Whilst, in the case of TL, such older dates might be explained by the reworking of chert artefacts from older deposits, the same would be very unlikely for OSL dated quartz mineral grains. The heavy burning of the sediment provides ideal conditions for the full resetting of the luminescence signal with little concern for potential issues pertaining to partial bleaching. Exposure to heat is also expected to greatly improve the sensitivity of the quartz for dating purposes. At Taforalt the latter was generally characterised by excellent response to artificial irradiation and samples always display perfect growth curves, low recuperation values as well as good recycling ratios.
Rather than the root of the problem being linked to the TL/OSL measurements themselves, the issue is more likely to stem from an incorrect estimate of the environmental dose rate. Indeed, the high concentration of ashy material incorporated into the Grey Series presents some specific challenges with regards to dosimetry. Elemental analyses of the sediment revealed very low concentrations of radioisotopes. In the case of OSL sample X1867 (**tab. 4.6**), they provided 0.42 % potassium, 9.8 ppm rubidium, 1.37 ppm thorium and

0.33 ppm uranium. These are responsible for very low external gamma dose rates ranging from 0.21 to 0.35 Gy/ka (based on OSL sample X1867 and TL samples X1866 and X2259).
The low concentrations of potassium may seem particularly surprising given the substantially higher concentrations of 1.17 % and 1.43 % recorded from samples X1864 and X1865 in the directly underlying Yellow Series. Wood ash, and leaf ash in particular, are also known to enhance considerably the concentration of potassium in soils (Ohno/Erich 1990) with wood ash generally containing c. 4 % of potassium. However, the high solubility of potassium in well drained coarse sediments, such as those forming the bulk of the GS, could also lead to depletion of ^{40}K over time, notably during prolonged periods of increased precipitation. Due to leaching in the past, the recorded modern values may thus not reflect the original concentrations and the calculated beta and external gamma dose rates may therefore not necessarily be reliable. A small increase of only 0.15 % to 0.20 % in the amount of potassium present within the sediment would be sufficient to bring most of the OSL and TL dates into alignment with the AMS ^{14}C dates. The unusual nature of the heavily burnt and powdery sediment may also require a downward revision of the mean sediment density which, for the purposes of most dose rate calculations, is generally assumed to be similar to compacted sand with values typically centred around 1800-1900 kg/m³. The bulk density of wood ash is considerably lower (i. e. 600-900 kg/m³) and, given the high occurrence of ashy debris contained within the GS, it seems reasonable to conclude that a lower value of c. 1200 to 1500 kg/m³ would provide a better approximation. The effect of this would be to further reduce the calculated age estimates. Further quantification of these effects will be required in order to provide more reliable luminescence age estimates for samples collected from the GS.